Electrochemical Properties of PVDF-Based Nanocomposite Solid Polymer Electrolytes

*Soo-Kyeong Jeong, Yu-Jin Lee, Nam-Ju Jo**

Summary: Poly(vinylidene fluoride) (PVDF)-based nanocomposite solid polymer electrolytes (NSPEs) were prepared and ion conduction property was investigated according to the filler content. The organically modified clay (Cloisite®15A, C15A) was used as a filler because it has had a good compatibility with PVDF. X-ray diffraction measurement revealed the dispersion of C15A in PVDF and the states of exfoliation and intercalation of C15A were also observed by transmission electron microscopy. In order to confirm the ion conduction properties of NSPEs with $LiCF_3SO_3$, ac impedance analyzer and FT-IR spectrometer were used. The highest ionic conductivity was appeared in NSPE containing 5wt% of C15A and the maximum conductivity was 1.04×10^{-3} S cm^{-1}. And the improvement of electrochemical stability of NSPEs by adding C15A was confirmed.

Keywords: electrochemical properties; nanocomposites; organoclay; poly(vinylidene fluoride); solid polymer electrolyte

Introduction

Investigations into lithium ion conducting solid polymer electrolytes are increased due to their potential use in various electrochemical applications, particularly those where high energy density is required, for example, electric vehicles and portable devices. Batteries based on polymer electrolytes also have the capabilities of outstanding performance in terms of mechanical stability, reliability and safety. However, there is a major drawback that they suffer from a relatively low ionic conductivity at room temperature.[1,2] Recently, the addition of inert nano-sized fillers within polymer electrolyte has attracted considerable attention due to their mechanical stability, ionic conductivity and electrolyte/electrode interface stability.[3,4] By introducing fillers in polymer electrolytes, it has an effect on the recrystallization kinetics of the polymer, thus local relaxation and segmental motion of polymer chains improve that allow efficient Li^+ transport.[5–7] Also, Croce et al.[8] suggested a multi-action role of the ceramic filler which involves scavenging, i.e. trapping the residual traces of impurities from the lithium-electrolyte interface, and shielding, i.e. favoring the formation of smooth and uniform passive layers. Kumar and Scanlon[9] suggested that the addition of nano-size ceramic filler having a high surface area suppresses the interfacial reaction between the lithium electrode and the polymer electrolyte by decreasing the contact area.

In this study, Poly(vinylidene fluoride) (PVDF)-based nanocomposite solid polymer electrolytes (NSPEs) were prepared using clay as the filler, which is consisted of stacked silicate layers having a high aspect ratio. PVDF, which has a strong electron withdrawing function and an unique arrangement, delivers a high dielectric constant ($\varepsilon = 8.4$).[10,11] In addition, using organoclay modified with organic modifier, it was expected that dispersity of clay and performance of NSPEs would increase because organoclay is endowed with good

Department of Polymer Science and Engineering, Pusan National University, San30, Jangjeon-dong, Gumjeong-gu, Busan, 609-735, Republic of Korea
Fax: (+82) 51 513 7720
E-mail: namjujo@pusan.ac.kr

affinity with hydrophobic PVDF.[12,13] Therefore, the structural factors contributing to ion conduction and the electrochemical performances by adding organoclay in NSPEs were investigated.

Experimental Part

Materials

Poly(vinylidene fluoride) (PVDF) with average molecular weight (Mw) of 534,000 was obtained from the Aldrich co. (USA) and used without further purification process. Organically modified clay, Cloisite® 15A (C15A) provided by Southern Clay Products Inc. (USA) and lithium trifluoromethanesulfonate ($LiCF_3SO_3$) (Aldrich co., 99.5%) was dried each in vacuum at 90°C overnight and stored in a desiccator under nitrogen. And N,N-dimethylformamide (DMF) (Junsei chemical co.) was used as an organic solvent to dissolve the materials.

Preparation of NSPEs

An appropriate amount of C15A was introduced into DMF and stirred for 72 h at 80°C and sonicated intermittently. And then calculated amounts of this solution were added to the prepared PVDF/DMF solution and stirred again for 24h until the solution was homogeneous. The PVDF/C15A nanocomposite films for the characteristic analysis of nanocomposite were prepared by solution casting method. Finally, a definitive amount of $LiCF_3SO_3$ was added to PVDF/C15A nanocomposite solution prepared previously and it was stirred again to homogenize for 12h. After mixing, the solution was directly cast on a 3×3 cm^2 stainless steel plate and allowed to dry in the vacuum system for 5 days at 30°C to remove the solvent perfectly. The thickness of the completed NSPE films was $50 \sim 100$ μm.

Characterization

Wide-angle X-ray diffraction measurements to confirm the dispersion of C15A in PVDF were carried out using Rigaku Model D/Max-2400 with Cu-Kα radiation ($\lambda = 1.5405$ Å) and operation was in the θ–θ geometry. The scanning range was from $2\theta = 1.5°$ to 30° with a rate of 1°/min. Transmission electron microscopy (TEM) images for acquiring a direct visualization of the particular layer characteristics of the nanocomposites were obtained by TEM (FEI tacnai 200) with an accelerating voltage of 200kV. The degree of crystallinity for each sample was obtained from differential scanning calorimetry (DSC, TA instrument Q100) measurements. Dry nitrogen gas was allowed to flow through the DSC cell at a rate of 40 ml/min. The samples were equilibrated at −60 °C and heated up to 200 °C at a heating rate of 10 °C/min, and held there for 3min in order to erase any previous thermal history. The glass transition temperature (T_g) was confirmed by dynamic mechanical analysis (DMA) using a TA instrument 4100 under a tension mode at a frequency of 1Hz. The temperature range was from −100 to 50 °C at a heating rate of 5 °C/min. The samples were thin rectangular strip with dimension of 20 mm × 5 mm × 0.2 mm. Ionic conductivity measurements of NSPEs were carried out using a Zahner Electrik IM6 impedance analyzer over the frequency range 1 MHz to 100 mHz in an argon atmosphere at room temperature. The samples were sandwiched between two stainless steel blocking electrodes (SS|NSPE|SS) with attached electric wires. FT-IR studies were performed at ambient temperature using Jasco 460 Plus FT-IR spectrometer with 2 cm^{-1} spectral resolution in the frequency range of 4000 and 400 cm^{-1} and FT-IR spectra were corrected to the same baseline. Deconvolution of the composite bands of the FT-IR spectra were accomplished by the best fits of constituent Gaussian peaks using Microcal Origin 7.0 software. The maximum error associated with the integrated band area of the deconvoluted FT-IR spectra is expected to be within ±5%. The electrochemical stability windows of NSPEs were studied using a linear sweep voltammetry (LSV) (Zahner

Electric IM6) in a potential range of 2 to 6V versus Li/Li$^+$ at a sweep rate of 5 mVs^{-1}. Stainless steel (SS304) was used as a working electrode and Li metal as both counter and reference electrode, respectively.

Results and Discussion

The Analysis of Characteristics in PVDF/C15A Nanocomposites

To verify the dispersion states of C15A in PVDF, XRD measurements were carried out and the results presented in Figure 1. The diffraction peak at $2\theta = 2.96^\circ$ is d_{001} plane peak in the layer structure and from intensity and shift of this peak, the dispersion state of clay was evaluated. When small amounts of C15A were added in PVDF, it was confirmed that C15A stacks were exfoliated in PVDF from the disappearance of C15A peak. In more than 5wt% content of C15A, the peak of C15A started to appear at shifted to low angles corresponding to an increase in the d-spacing from 3.0 to 3.6 nm. It indicates that hydrophobic PVDF chains were easily intercalated into relatively hydrophobic C15A due to having analogy property between PVDF and C15A. In the high content as well as in the low content of C15A, the intercalation was occurred but the intensity of C15A peak increased with C15A contents. From this result, it could be expected that the thicker C15A stacks rather than dispersed C15A with an increase of C15A content were presented partially and the interactions among PVDF, C15A, and Li salt were decreased to some extent.

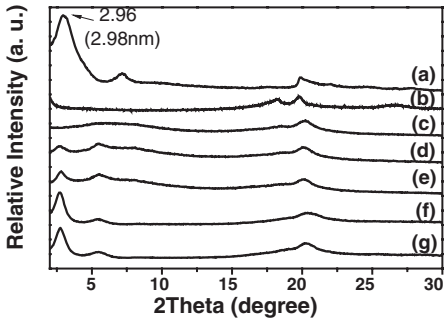

Figure 1.
X-ray diffraction (XRD) patterns of (a) C15A, (b) PVDF, and PVDF/C15AX nanocomposite materials; $X = (c)$ 1wt%,(d) 3wt%, (e) 5wt%, (f) 7wt%, (g) 9wt%.

Also, the crystalline peak of PVDF at $2\theta = 18.7^\circ$ and 20.5° showed far broader and weaker intensity due to the addition of C15A. And the broad peak near $2\theta = 20^\circ$ may be appeared from the C15A and PVDF crystalline peak together. As a result, not only exfoliated and intercalated C15A but C15A stacks contributed to the destruction of PVDF crystalline structure.

Figure 2 shows TEM images of PVDF/C15A nanocomposites containing 3wt% and 5wt% of C15A. The dark lines in Figure 2 represent the individual clay platelet. The sample containing 3wt% of C15A in Figure 2(a) shows the co-existing of exfoliated and intercalated structures. In case of 5wt% of C15A as shown in Figure 2(b), it was confirmed that the regular intercalated structures were achieved effectively. Thus, TEM observations revealed the states of clay platelets visually as considered previously in XRD studies.

The degree of crystallinity (X_c) and glass transition temperature (T_g) of the nanocomposites were measured to analyze the changes of the nanocomposite structure by the addition of C15A in PVDF and showed in Figure 3. X_c reduced dramatically as C15A contents increased. It could be known that the addition of C15A in PVDF interrupted crystallization and fraction of free volume of amorphous region was increased.

T_g of the nanocomposites showed tendency to decrease as C15A contents increased, which may be attributed to the plasticization effect of C15A.[14] These results will provide beneficial environment to move of Li$^+$ ion related to ionic conductivities of NSPEs.

Ionic Conductivity

Figure 4 presents the ionic conductivity of PVDF-based NSPEs with different C15A

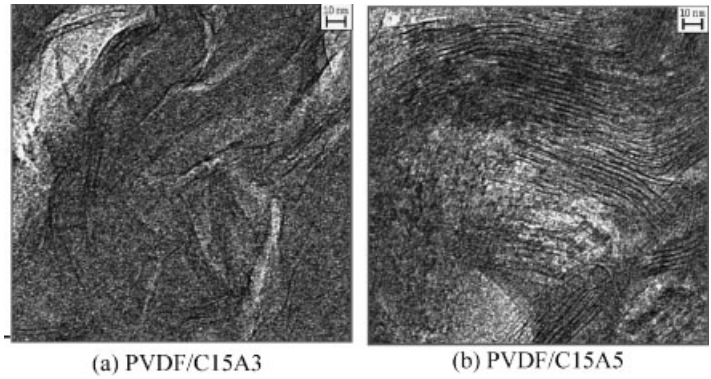

Figure 2.
TEM images of PVDF/C15A nanocomposites containing (a) 3wt% of 15A and (b) 5wt% of C15A.

and Li salt contents. Ionic conductivity of NSPE increased with salt concentration. Also, the ionic conductivity of NSPE increased as C15A contents increased up to 5 wt%, whereas it decreased continuously more than 7 wt% of C15A contents. Consequently, NSPE with 5 wt% of C15A had the highest ionic conductivity at the same salt concentration. As mentioned previously, C15A was well dispersed in PVDF and the free volume available for segmental motion of PVDF was expanded. Also, negative charges on dispersed organoclay layers were helpful to let the Li ion move easily as same as the polar group of PVDF. But in content of C15A more than 7 wt%, ionic conductivity decreased even though the degree of crystallinity and T_g of nanocomposites decreased. This may arise from that the partially presented C15A stacks reduce the interaction between silicate layers and Li salts and function as obstacle in moving Li ion smoothly. A maximum conductivity of 1.04×10^{-3} Scm^{-1} was obtained at room temperature for PVDF/C15A5 with 40wt% of salt in this system.

FT-IR Analysis

FT-IR spectroscopic measurement is powerful tool for probing the microscopic details and confirming the presence of free ions, ion pairs and aggregates in SPEs. Clear distinction between free ions, contact ion pairs, and higher aggregates is observed

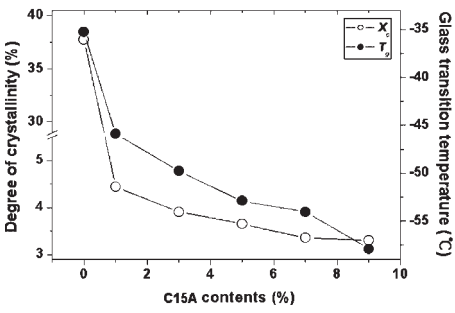

Figure 3.
Degree of crystallinity by DSC and glass transition temperature by DMA according to C15A contents in PVDF/C15A nanocomposite materials.

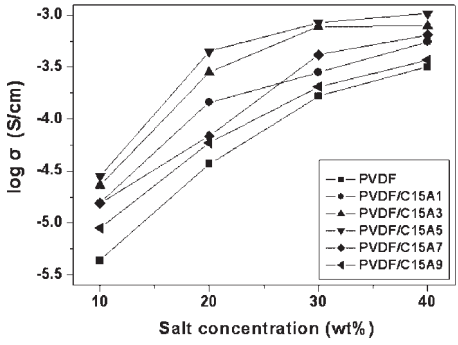

Figure 4.
Ionic conductivity as a function of salt concentration of PVDF-based NSPEs with various C15A contents.

in vibrational spectra of the internal mode of anions, such as the $CF_3SO_3^-$ ion. In particular, the characteristic symmetric SO_3 internal modes of the $CF_3SO_3^-$ anion are sensitive to the change in the coordination state of the anion. Thus, the peak fitting of these regions has provided information of the types of free ions and ion aggregates in SPEs.[15–17]

From the peak fitting results, we could obtain the fraction of each salt form, free ions and ion aggregates, in salt concentration from 10 to 40 wt% as shown in Figure 5. As the salt concentration increased, the fraction of free ions reduced and ion aggregates increased simultaneously, because the average inter-ionic distance decreased and ionic interaction increased. As considering the tendency of ionic conductivity, partially formed ion aggregates even at the maximum salt concentration up to 40wt% had no effect on the decrease of ionic conductivity and the movement of free ions.

To verify the number of charge carriers, an important factor contributed to ionic conductivity of PVDF-based NSPEs, quantitative analysis was performed for all samples by using FT-IR absorption spectra. For the quantitative analysis of free ions, two peaks of FT-IR spectra, 'free ion' peak (1032 cm^{-1} of wavelength[15]) in $LiCF_3SO_3$ (P1) and fixed CH_2 bending peak (1400 cm^{-1} of wavelength[18]) in PVDF (P2) which isn't affected by surrounding environments, were taken, and the ratio of P1 to P2 intensity was calculated. Figure 6 shows the result of quantitative analysis of free ions for NSPE with 40wt% Li salt representatively. Relative quantity of free ion increased up to 5wt% of C15A contents because the negative charges on organoclay layers assist the ionization of the lithium salt. But it was decreased to some extent for the C15A contents more than 7wt%. It could be thought that the partially presented C15A stacks reduced the interaction between organoclay layers and Li salts contributed to salt ionization. From above results, it could be concluded that NSPE containing 5wt% of C15A possessed the largest number of charge carrier, and above that content, C15A stacks started to act as barriers and interrupted the movement of Li ion smoothly.

Electrochemical Stability

Electrochemical stability of the polymer electrolyte in contact with the electrode material is an essential parameter for providing satisfactory performance in practical applications and the electrochemical stability window of at least 4V is needed to accommodate overcharge and discharge reactions.[19] Figure 7 shows the linear sweep voltammogram of NSPE containing

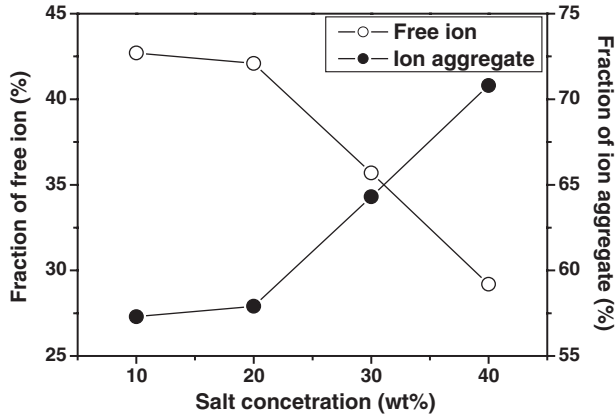

Figure 5.
The fraction of free ions and ion aggregates in PVDF-based SPE with various salt concentration.

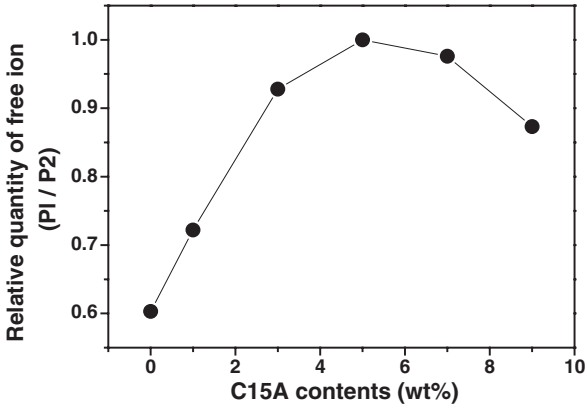

Figure 6.
Relative quantity of free ions in NSPEs with 40wt% salt at various C15A contents.

5wt% of C15A and SPE without C15A at the same salt concentration. Electrochemical stability window was determined as the potential at a rapid increase in current. Pure SPE without C15A was started to occur the anodic decomposition in more than 3V slightly and increased rapidly in near 4.73V, whereas the NSPE containing C15A was stable until reaching the potential limit to 5.136V. Thus, the electrochemical stability of PVDF-based NSPE was improved in comparison with pure SPE, which indicated that NSPE was less reactive towards electrode by the action of C15A used as the filler.

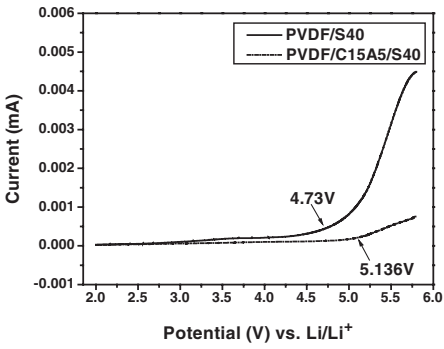

Figure 7.
Linear sweep voltammogram of PVDF-based NSPE.

Conclusions

PVDF-based NSPEs were prepared by dispersing organoclay (Cloisite®15A, C15A) and evaluated using XRD, TEM, DSC, DMA, ac impedance, FT-IR, and LSV. By XRD data and TEM images, it could be confirmed that clay was dispersed well in the NSPE up to 3 wt% of C15A but clay stacks started to be aggregated in more than 5 wt% content of C15A. Dispersed clay played a role of increasing free volume available to segmental motion of PVDF and movement of Li ion. The highest ionic conductivity of 1.04×10^{-3} Scm^{-1} showed up in the NSPE with 5 wt% of C15A. This result was caused by not only the increase of free volume but also the number of charge carriers caused by the increase of interaction between clay and Li salt. In more than 7 wt% of C15A contents, ionic conductivity decreased contrarily because partially presented C15A stacks acted as barriers and interrupted the movement of Li ion despite of low degree of crystallinity and glass transition temperature, and large number of charge carriers. Also, NSPE containing C15A showed higher electrochemical stability than pure SPE. From these points of view, PVDF-based NSPEs are good candidates for rechargeable lithium batteries.

Acknowledgements: Authors would like appreciate financial support by grant no. R01-2003-000-11612-0 from the Basic Research Program of the Korea Science & Engineering Foundation. This work was also supported by the Brain Korea 21 Project.

[1] F. M. Gray, "*Solid Polymer Electrolytes: Fundamentals and Technological Applications*", VCH Publishers, New York 1991, p. 1.
[2] P. G. Bruce, *Chem. Commun.* **1997**, *19*, 1817.
[3] F. Croce, G. B. Appetecchi, L. Persi, B. Scrosati, *Nature* **1998**, *394*, 456.
[4] F. Croce, R. Curini, A. Martinelli, L. Persi, F. Ronci, B. Scrosati, R. Caminiti, *J. Phys. Chem. B* **1999**, *103*, 10632.
[5] C. C. Liang, *J. Electrochem. Soc.* **1973**, *120*, 1289.
[6] J. E. Weston, B. C. H. Steele, *Solid State Ionics* **1982**, *7*, 75.
[7] B. Kumar, L. G. Scanlon, *Solid State Ionics* **1999**, *124*, 239.
[8] F. Croce, L. Persi, F. Ronci, B. Scrosati, *Solid State Ionics* **2000**, *135*, 47.
[9] B. Kumar, L. G. Scanlon, *J. Power Sources* **1994**, *52*, 261.
[10] H. S. Choe, J. Giaccai, M. Alamgir, K. M. Abraham, *Elecrochimica Acta* **1995**, *40*, 2289.
[11] C. Y. Chiang, Y. J. Shen, M. J. Reddy, P. P. Chu, *J. Power Sources* **2003**, *123*, 222.
[12] J. H. Park, S. C. Jana, *Macromolecules* **2003**, *36*, 2758.
[13] V. Krikorian, D. J. Pochan, *Chem. Mater.* **2003**, *15*, 4317.
[14] C. R. Tseng, J. Y. Wu, H. Y. Lee, F. C. Chang, *Polymer* **2001**, *42*, 10063.
[15] W. Huang, R. Frech, R. A. Wheeler, *J. Phys. Chem.* **1994**, *98*, 100.
[16] D. R. MacFarlane, *Electrocimica Acta* **1995**, *40*, 2333.
[17] A. G. Bishop, D. R. MacFarlane, D. McNaughton, M. Forsyth, *Solid State Ionics* **1996**, *85*, 129.
[18] Pavia, Lampman, G. M. Kriz, "*Inrtoduction to Spectroscopy*", Harcourt College Publishers, Orlando 2001, p. 28.
[19] Z. Gadjourova, Y. G. Andreev, D. P. Tunstall, P. G. Bruce, *Nature* **, 2001**, *412*, 520.

